Nano Co_3O_4/NiO Catalysts Pyrolysis of *Cotinus nana* Bark for Bio-oil and Biochemicals Raw Material

Junwei Lou,[a] Xiaochen Yue,[b,*] and Yafeng Yang [b,*]

Cotinus nana W. W. Smith is a valued landscape shrub and a good afforestation species that is also widely used in the pharmaceutical industry. In this study, the use of *Cotinus nana*'s bark (CNB) as biofuel and a biochemical under the catalysis of nano-Co_3O_4/NiO was explored by various thermogravimetric methods and Fourier transform infrared (FTIR) analysis. The bark powder was extracted using a methanol/benzene solution, and then analyzed by FTIR and gas chromatography-mass spectrometry (GC-MS). The results showed that the pyrolysis products of CNB are rich in phenols, alcohols, and biofuels. The Co_3O_4 and NiO act as nanometal catalysts in the release of pyrolysis gases, accelerating the precipitation of gaseous products. Among them, NiO has the most obvious catalytic effect in the pyrolysis process of the material components. At the same time, in the temperature range of 40 to 850 °C, as the pyrolysis rate of the sample increases, the pyrolysis process becomes more intense. In contrast, the contents of the extracts N,N-diethyl-formamide, butyric acid, and oleic acid are not only widely used in industry, but also play a pivotal role in medicine. Therefore, the bark of *Cotinus nana* is an excellent plant material for biofuels and biochemicals.

DOI: 10.15376/biores.18.1.678-700

Keywords: Cotinus nana; TG-FTIR; PY-GC-MS; Nano Co_3O_4/NiO catalysis; Biochemical; Biofuel

Contact information: a: School of Architectural Engineering, Zhejiang Business Technology Institute, Ningbo 315012, China; b: School of Forestry, Henan Agricultural University, Zhengzhou 450002, China; Corresponding authors: yuexiaochen95@163.com; yangyafengzz@163.com

INTRODUCTION

With the rapid expansion of the social economy, the global demand for energy is increasing rapidly. Over-reliance on progressively depleted fossil energy, especially petroleum energy, has seriously affected the continued development of the national economy. Therefore, the development of new renewable alternative energy sources has become an important way to alleviate energy shortages and reduce environmental pressures.

Biomass energy has its value in human life and social activities due to its rich resources, renewable nature, and lack of associated air pollution emissions (Gu *et al*. 2018). In the process of using biomass as an energy source, it is first converted into liquid fuel with high energy density by the thermochemical conversion process, which greatly increases the benefit and facilitates storage and transportation (Mekonnen *et al*. 2017; Wiklund *et al*. 2017). Different biomass feedstock yields different biomass liquefaction products. The liquid fuel products are primarily bio-oil, biodiesel, ethanol, and dimethyl ether, which can replace petroleum energy products and become alternative fuels for vehicles. Biomass energy products have broad application space for technology

development due to their performance advantages. With the continuous breakthrough in the research of gasification, oil, and hydrogen productions, the manufacture of cleaner and cheaper energy is of great significance for the effective use and sustainable development of energy.

As an organic substance formed by natural growth, wood contains other small chemical components, in addition to the main components of cellulose, hemicellulose, and lignin. These minor components are generally called extracts, leaching components, and inclusions. Wood extract is a general term for substances extracted with organic solvents such as methanol, ethanol, benzene, dichloromethane, acetone, or water. It is abundantly present in resin channels, gum roads, and parenchyma cells. The composition is very complex. The content and chemical composition also vary depending on the tree species, location, origin, harvesting season, storage time, and extraction method (Baruah *et al*. 2015; Luís *et al*. 2016; Sánchez-Gómez *et al*. 2017). It has been identified that wood extracts generally contain more than 700 compounds, such as tannins, resins, gums, essential oils, pigments, fats, sugars, and starches, some of which are important raw materials for the chemical, pharmaceutical, and other industrial sectors and have a certain economic value. For example, a unique anti-cancer effect of paclitaxel was obtained from the bark of *Taxus wallichiana* var. *chinensis*, which has been shown effective in many clinical trials against leukemia, breast cancer, ovarian cancer, lung cancer, melanoma cancer, and colon cancer (Banerjee *et al*. 2016; He *et al*. 2016; Kim *et al*. 2016; Yu *et al*. 2016).

Cotinus nana W. W. Smith is a member of the Anacardiaceae family. It has been used as a shelter forest tree for water and soil conservation and as a landscaping plant. There are many reports available on its cultivation research. Since the wood of *Cotinus nana* is yellow, yellow industrial dyes can be obtained by extracting it. In recent years, many pharmacodynamic tests have shown that it has antibacterial, anti-hepatitis, anti-fatigue, anti-coagulation, and other effects. It can be used to treat colds, high blood pressure, jaundice, *etc*. (Matic *et al*. 2013; Lei *et al*. 2015; Ilczuk *et al*. 2016; Matic *et al*. 2016). Exhaustive studies have been carried out on the flavonoids present in *Cotinus nana* as active ingredient. The results showed that *Cotinus nana* could significantly shorten the length of thrombus, reduce the wet and dry weights of thrombus, reduce the thrombus index, prolong the thrombin time, and show obvious anticoagulant and antithrombotic effects.

The extract from *Cotinus nana* has a scavenging effect on free radicals. Reddy *et al.* (2005) studied the antioxidant activity of the dried part of *C. nana* by total antioxidant assay, DPPH free radical scavenging, and anti-lipid peroxidation (LP), revealing the antioxidative effect of *C. nana* is positively correlated with the polyphenols content (Reddy *et al*. 2005; Marcetic *et al*. 2012). Ivanova *et al.* (2005) screened various plants in Bulgaria and investigated the *in vitro* antioxidant activity of *C. nana* leaf water extract (Ivanova *et al*. 2005). The results showed that it had good antioxidant activity. *Cotinus nana*'s extract also revealed certain anticoagulant effects. Matic *et al.* (2011) have studied the blood clotting time, *in vitro* thrombus, prothrombin time, thrombin time to calculate thrombus index, and platelet adhesion rate in rats with acute blood stasis model (Matic *et al*. 2011). The results showed that *C. nana* can shorten the length of the thrombus, reduce the wet and dry weights of the thrombus, reduce the thrombus index, and prolong the thrombin time (Matic *et al*. 2011). The flavonoids from *C. nana* also have a certain antihypertensive effect. Demirci *et al.* (2003) evaluated the blood pressure lowering effect of *C. nana* in domestic dogs (Demirci *et al*. 2003). The results showed that the water extract of *C. nana*

had obvious antihypertensive effect (Demirci *et al*. 2003). The antibacterial activity of leaf volatile oil and shoot extract has also been reported. Jassbi *et al.* (2002) extracted volatile oil from the leaves of *Astragalus* membranes by steam distillation and studied its antibacterial activity. Studies have found that its antifungal effect is higher than the commonly used antifungal agent bifonazole (Jassbi *et al*. 2002; Peng *et al*. 2016). Ge *et al.* (2022) studied the micromolecules of the extracts and pyrolysis products of *Pinus armandii* by GC-MS, PY-GC/MS and NMR. The active molecular compounds of *Pinus armandii* have good development and application prospects.

For the *Cotinus nana* species, recent studies on its shoots, leaves, and flowers have been extensive and in-depth. However, the physiological role of the bark of *C. nana* in medical industries has not been studied in depth. In this paper, *Cotinus nana* bark (CNB) was used as the research object. The bark in fast gasification to yield bio-oil catalyzed by nano-Co_3O_4 and nano-NiO, and the extraction of bioactive drug molecules were investigated. The catalytic effects of nano-Co_3O_4 and nano-NiO on CNB were analyzed by pyrolysis gas chromatography-mass spectrometry (PY-GC-MS), thermogravimetric analysis (TG-DTG), and thermogravimetric-infrared (TG-IR). The gas chromatography-mass spectrometry (GC-MS) and Fourier transform infrared (FTIR) methods were used to analyze the medical and health functions of the ingredients and bioactive substances of the CNB extract. CNB was explored as premium raw material for biochemicals *via* nanocatalysis and extract studies.

EXPERIMENTAL

Experimental Materials

The bark of *Cotinus nana* was obtained from the Xiaoqinling National Nature Reserve in Henan Province, China. The procedure was to peel the bark of the sample from the wood, freeze dry the separated bark, use a flour mill to break the bark, pass a 120-mesh sieve, and put the screened fine powder into a vacuum dryer for test detection. Then 30 g of CNB powder was weighed and methanol/benzene (1:1) solvent was used for extraction to obtain the extracts. The amount of organic solvent was 300 mL, the extraction time was 4 hours, and the extraction temperature was 60 ℃. Finally, use the rotary evaporator to concentrate to 30 mL to obtain the extracts.

Nanocatalysts Co_3O_4 (30 nm) and nanocatalysts NiO (30 nm) each with a purity of 99.5% were prepared by the Macklin company (Macklin, Shanghai, China). The bark sample was dried, broken into 20-g pieces, and then divided into four 5-g portions. The first 5-g CNB piece was called HP1; 0.05 g nano-Co_3O_4 and 5 g CNB powder were uniformly mixed, named HP2; 0.05 g nano-NiO and 5 g CNB powder were uniformly mixed, named HP3; 0.025 g nano-Co_3O_4, 0.025 g nano-NiO, and 5 g CNB powder were uniformly mixed named HP4.

Table 1. Optimization of the Experimental Program

No.	Solvent (mL)	M (g)
B1	Methanol/ Benzene (1:1) 300	30.0

Table 2. Optimization of the Experimental Program

No.	Material	Catalyst
HP1	Bark sample (5 g)	-
HP2	Bark sample (5 g)	Co_3O_4 (0.05 g)
HP3	Bark sample (5 g)	NiO (0.05 g)
HP4	Bark sample (5 g)	Co_3O_4 (0.025 g) / NiO (0.025 g)

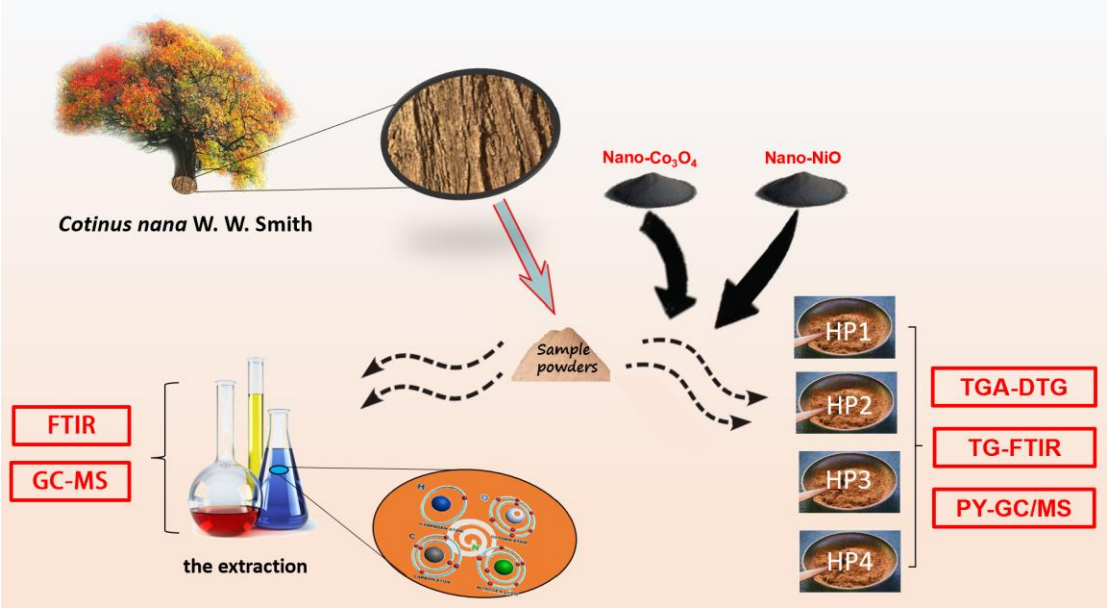

Fig. 1. Experimental flow chart

Experimental Methods

TGA-DTG experiments

The powders of the bark samples were analyzed using a thermogravimetric analyzer (TGA-Q500, TA Instruments, New Castle, Delaware, USA). The temperature program started at 30 °C and was increased to 850 °C at heating rates of 25 °C/min and 55 °C/min, respectively (Kim 2013; Doss *et al*. 2017).

TG-FTIR experiments

The analysis of the HP1, HP2, HP3, and HP4 samples was performed using the thermogravimetric analyzer listed above (TGA Q500, TA Instruments) connected to a Fourier-transform infrared spectrometer (Thermo Scientific Nicolet™ 6700, New Castle, Delaware, USA). The temperature was increased from 50 to 850 °C at 55 °C/min. The IR spectra were recorded at 4,000 to 400 cm^{-1} with a resolution of 1.0 cm^{-1}. Three-dimensional (3D) FTIR spectrograms were obtained (Bassilakis *et al*. 2001; Jong *et al*. 2003; Zhu *et al*. 2008; Jiang *et al*. 2010).

PY-GC-MS analysis

The powdered HP1, HP2, HP3, and HP4 samples were analyzed using a CDS 5000-Agilent 7890B-5977A (Palo Alto, California USA) Py-GC-MS system. High purity helium was used as carrier gas, the pyrolysis temperature 850 °C was used at the rate of 20 °C/ms, and pyrolysis time was 15 s. The pyrolysis transfer line and the injection valve temperature were set to 300 °C; the capillary column measured 30 m × 0.25 mm × 0.25 μm; shunt mode, split ratio was 50:1, and shunt rate was 50 mL/min. The GC program temperature started at 40 °C for 2 min, increased to 120 °C at a rate of 5 °C/min, and then increased to 200 °C at a rate of 10 °C/min, kept for 15 min (Zodrow *et al*. 2002; Dong *et al*. 2012; Kaal *et al*. 2012; Xue *et al*. 2017).

FTIR analysis

The FTIR spectra of the extracted samples were obtained using a Thermo Fisher Scientific iS10 FTIR spectrophotometer (Shanghai, China) (Byler and Susi 2010; Camacho *et al*. 2015).

GC-MS analysis

GC/MS determination: Samples were analyzed using GC-MS (Agilent7890B-5977B, Agilent Technologies, Palo Alto, California USA). The column used was HP-5MS (30 m × 250 μm × 0.25 μm). The carrier gas used was high purity helium at the flow rate of 1.0 mL/min, and the diversion ratio was 2:1. The temperature program for GC started at 50 °C, increased to 250 °C at a rate of 8 °C/min, then increased to 280 °C at a rate of 5 °C/min, and was retained for 4 min.

Mass spectrometry: The program scanned mass ranges from 30 amu to 600 amu, at ionization voltage 70 eV and ionization current 150 μA. Ion source and quadrupole temperatures were set to 230 °C and 150 °C, respectively (Fischer and Sauer 2003; Dauner and Sauer 2010; Jiang *et al*. 2017; Zhang *et al*. 2019).

RESULTS AND DISCUSSION

TGA-DTG Analysis

Thermogravimetric analysis is a commonly used test method in research and development and quality control (Wang *et al*. 2008; Chen *et al*. 2014). To understand the thermal stability of CNB and the combustion properties of its components, TGA-DTG analysis was used. Figure 2 shows the weight loss of bark powder at a heating rate of 25 °C/min. Figure 3 shows the weight loss of bark powder at 55 °C/min heating rate. The TGA-DTG weight loss data are shown in Table 3.

Figure 2 shows the TG curves of four groups of samples at 25 °C/min. The weight loss of sample HP1, HP2, HP3 and HP4 decreased from 100% to 27.9%, 27.4%, 17.9%, and 28.6%, respectively. Overall, the TG curve decline was divided into three phases. The first stage occurred at 30 to 200 °C, and this stage is the drying stage. Water was evaporated before 120 °C, and the small molecular volatile components started to thermally decompose. The weight loss rate of sample HP1, HP2, HP3 and HP4 process was 11.6%, 11.5%, 11.3%, and 9.8%, respectively. It can be seen from the DTG curve that the nanocatalyst had no obvious catalytic effect on the process. The DTG curve peaked as the initial moisture material evaporated and then gradually decreased.

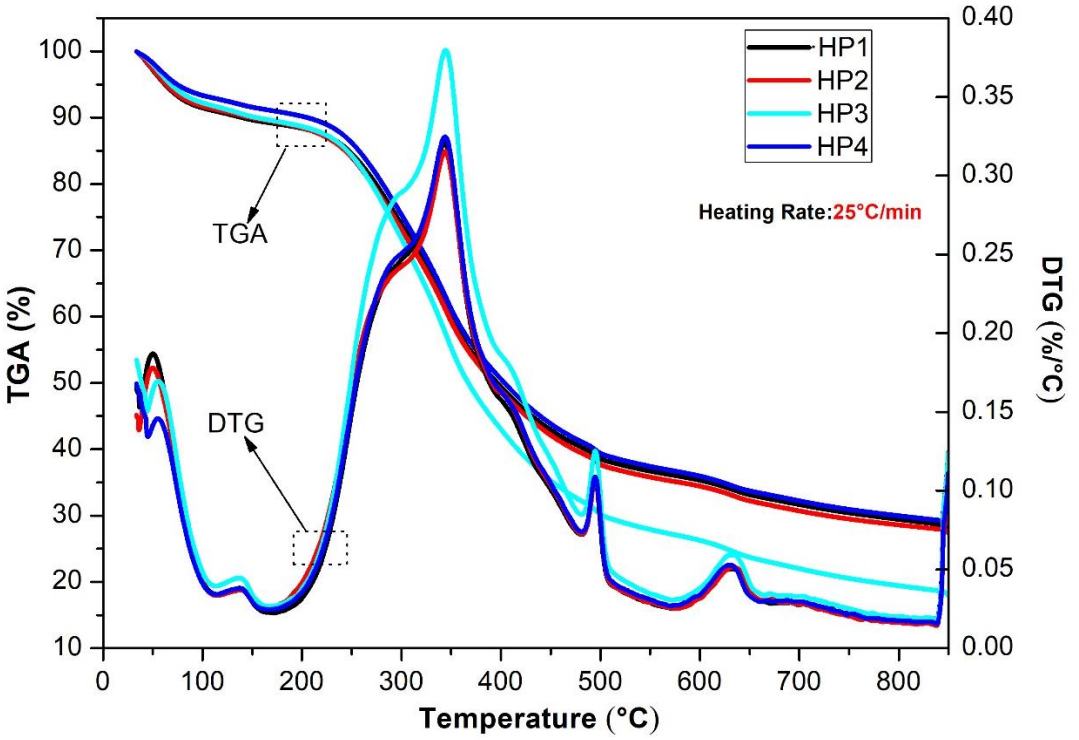

Fig. 2. TGA and DTG curves of the samples at a heating rate of 25 °C/min

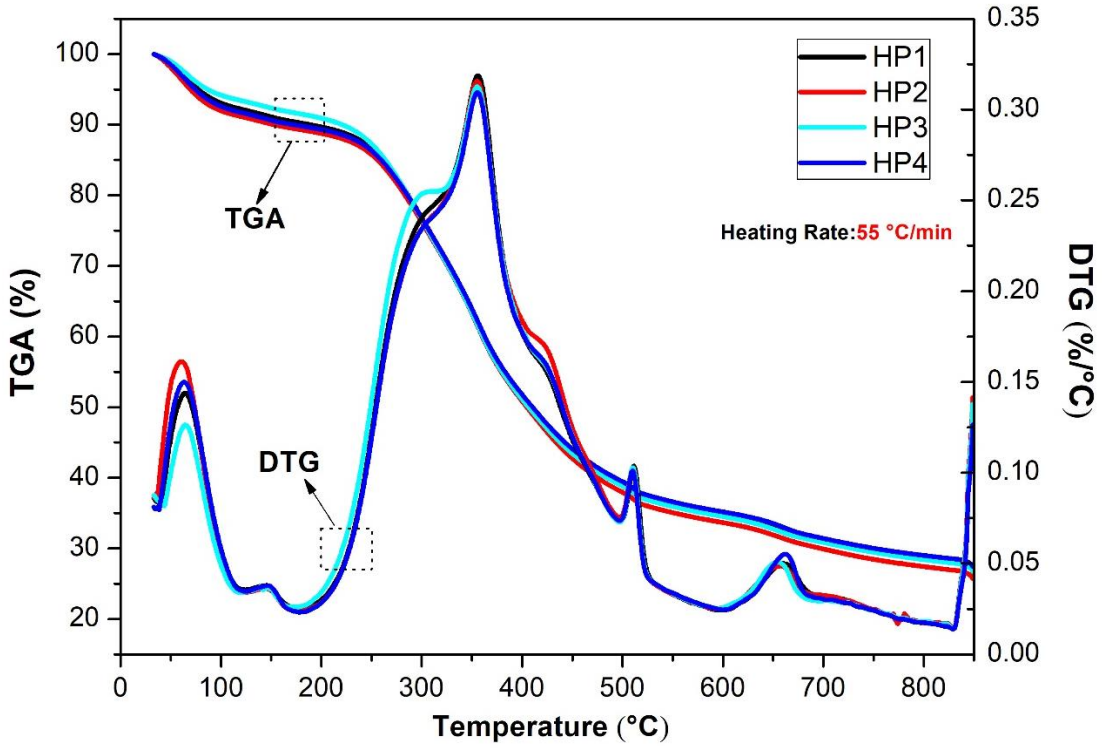

Fig. 3. TGA and DTG curves of the samples at a heating rate of 55 °C/min

Table 3. TGA-DTG Weight Loss Data of the Samples

W % / *T* °C	25 °C/min				55 °C/min			
	HP1	HP2	HP3	HP4	HP1	HP2	HP3	HP4
200	88.4	88.48	88.65	90.19	89.67	88.75	90.9	89.29
400	49.43	48.84	42.89	50.51	51.07	50.83	50.93	51.63
600	35.33	34.43	26.25	35.95	34.7	33.65	34.49	35.16
800	29.42	28.59	19.43	29.97	28.54	27.43	28.42	29

Notes: W: Weight; T: Temperature.

The second stage occurred at 200 to 500 °C. This stage involves volatilization and combustion℃. A large amount of volatilization is analyzed and burned, thereby mainly destroying non-covalent bonded molecules inside the sample. The heat generated by combustion further aggravates the combustion reaction, and then forms a significant weight loss peak. The weight loss of this process was 61.4%, 62.3%, 69.9%, and 60.6%, respectively. The DTG curve reached its maximum at 343 °C. From the weight loss rate and the DTG curve at this stage, the pyrolysis of the sample HP3 remarkably accelerated. This indicated that the nano metal catalyst NiO catalyzed the pyrolysis of the bark at this stage and accelerated the precipitation of volatile components. The third stage occurred from 500 to 850 °C, which is the coke combustion stage. As the temperature continued to rise after 500 °C, the volatile components burned out, the molecular structure of the sample underwent depolymerization and decomposition, the coke formed in the second stage began to burn, and the DTG curve also formed a second smaller peak. Weight loss peak then gradually decreased to zero. Compared with the four groups of samples, NiO exhibited the most obvious catalytic effect in the pyrolysis process of the material components. On the one hand, the rate of pyrolysis was accelerated, which was mainly reflected in the second stage. On the other hand, the sample had the least amount of pyrolysis residue and more pyrolysis occurred. The other catalyst Co_3O_4, had no obvious catalytic effect.

Figure 3 shows the TG curves of four groups of samples at 55 °C/min. When the heating rate was changed, the sample TG curve showed a high degree of coincidence and the shape was basically the same, but the heating rate had different effects on the pyrolysis weight loss process of each sample. The TG curves of sample HP1, HP2, HP3 and HP4 decreased from 100% to 26.8%, 25.7%, 26.7%, and 27.4%, respectively. When comparing the two sets of images, increasing the heating rate will lead to an increase in the maximum release rate of volatiles. The maximum release rate of volatiles corresponds to an increase in temperature, the pyrolysis rate of the sample increases, and the pyrolysis process becomes more intense (Williams and Besler 1996; Haykiri-Acma *et al*. 2006; Onay 2007). There was no significant difference between HP1, HP2, HP4, and HP3 curves, which indicates that the increase of heating rate was more catalyzed by pyrolysis than by the catalyst.

TG-FTIR Analysis

The 3D-FTIR spectra for the pyrolysis volatiles are shown in Fig. 4 for the HP1, HP2, HP3, and HP4 samples. Biomass pyrolysis technology is one of the main ways of thermochemical conversion and utilization of biomass. It is a process in which biomass is heated sufficiently to produce solid char, condensable liquid, and gas products in an oxygen-free or low-oxygen environment. The TG-FTIR technique was used to analyze the mass change characteristics of the sample pyrolysis gasification process and to quickly

analyze the formation and characteristics of gaseous product released. Figure 5 shows the cleavage of chemical bonds and the release of other small molecules of each sample during the gradual increase in temperature. It can be seen from the product precipitation spectrum that the characteristic peak corresponding to water vapor in the band of 3900 to 3700 cm^{-1} in the initial stage of pyrolysis, which indicates that the sample first releases the physically absorbed water in the initial stage of pyrolysis. It indicates also the cleavage of OH bonds in cellulose and hemicellulose, and the desorption process of free water.

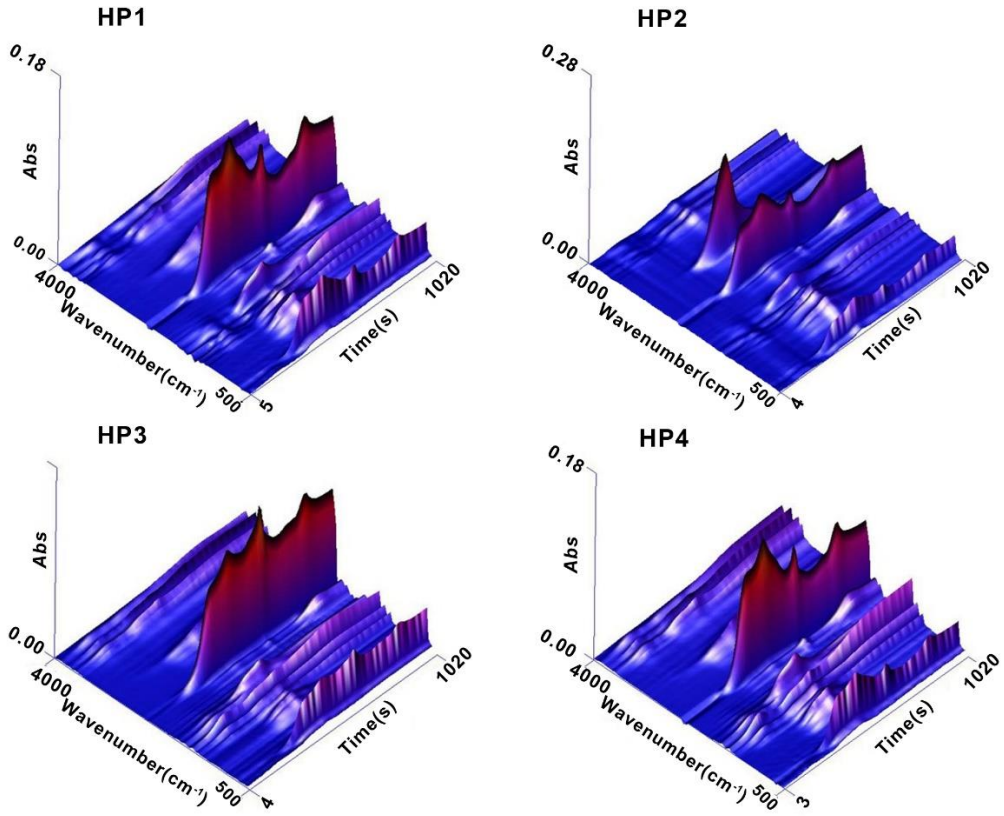

Fig. 4. 3D FTIR spectrograms of the samples: HP1, HP2, HP3, and HP4

As the temperature continued to rise, the band reached a distinct peak at 2450 to 2200 cm^{-1}. This corresponds to a macromolecular part involving C-H stretching vibration, C=O stretching vibration, C-H in-plane bending vibration, C-O and C-C skeleton vibrations, and the like, and various hydrocarbons, aldehydes, alcohols, and carboxylic acids formed. The main components released were CO_2 and CO gases. In the 2000 to 1300 cm^{-1} band, the main stretching vibrations were those of N=O, C-H, and S=O bonds, which were associated with a small amount of NO_2, SO_2, and some alkane gases (Meent *et al*. 1980; Chen *et al*. 2003; Mullen *et al*. 2013; Ephraim *et al*. 2018). In this process, the thermal decomposition of carbon is a main process in which the C-H bond and the C-O bonds are further broken and aromatized, and a graphite structure is gradually formed. The precipitation of CH_4 gas mainly occurred in the initial stage of pyrolysis, and a small amount of CH_4 was released at the initial stage of pyrolysis.

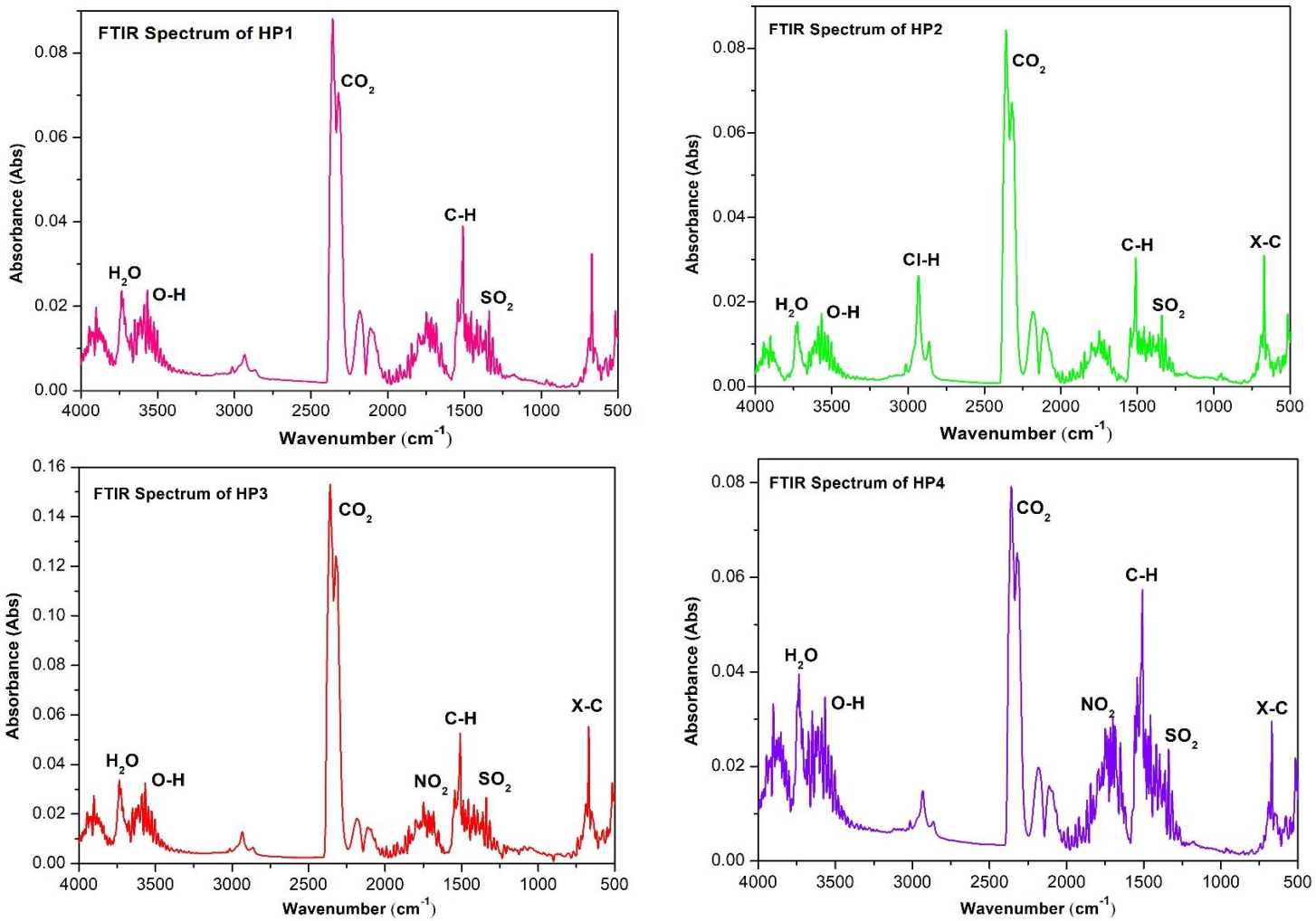

Fig. 5. FTIR spectrum of pyrolysis products from HP1, HP2, HP3, and HP4

As the pyrolysis temperature increased, the amount of CH_4 reached the maximum at 280 to 400 °C, which was due to the fracture of the O-CH_3 functional group. A weak gas release peak appeared at approximately 500 °C in the late stage of pyrolysis, presumably due to the secondary decomposition of organic substances, such as aldehydes, alcohols, acids, and ketones, in the process. The chain breakage and reforming reaction caused this phenomenon. Upon comparing the gas release peak of H_2O, CO, and CO_2 at the same heating rate, under the same conditions, the peak due to CH_4 was the smallest. CH_4 is a non-polar molecule with a tetrahedral structure, and may be released in the process of pyrolysis. The CO_2 is involved in the reforming reaction. Through careful comparison, the peaks corresponding to organic compounds, such as aldehydes, acids, and lipids, in these gas phase products are noticeable higher than other non-condensable gases. This shows that the proportion of these organic gases in the gas phase products was greater than that of non-condensable gases.

Based on the above analysis, the pyrolysis gasification process of the sample is mainly divided into two stages: volatilization pyrolysis of light components (low boiling point) at low temperature and pyrolysis gasification and condensation of heavy components (high boiling point) at high temperature (Tian *et al*. 2016; Si *et al*. 2018). Comparing the gas release peaks of the four groups of samples, it can be seen that HP2 added to the nano-catalyst Co_3O_4 was compared with the original powder HP1, and the Cl-H bond absorption peak was detected, indicating that the catalyst Co_3O_4 catalyzed the precipitation of HCl gas. Compared with the original powder HP1, the HP3 sample with NiO had a noticeably higher absorption peak of C=O bond, indicating that the catalyst NiO catalyzed the organic matter in cellulose, hemicellulose, and lignin to be volatilized by heat, and rapidly released large amounts of CO_2 gas. The rate of loss of weight gradually reached its maximum, and the peak of CO_2 absorbance also reached its maximum at this stage. Compared with HP1, HP4 with both catalysts increased the absorption peaks of OH bond, CH bond, and N=O bond, indicating that pyrolysis was simultaneously carried out by adding catalysts Co_3O_4 and NiO during pyrolysis. The production of process gas materials had the best catalytic effect. Furthermore, the size of the metal nanoparticles largely affected their catalytic function, and future TG-FTIR studies can begin by changing the type of catalyst and reducing the particle size of the catalyst (Mahmoud *et al*. 2010; Liu *et al*. 2016; An *et al*. 2017).

PY-GC-MS Analysis

The total ion current chromatograms of the samples from PY-GC-MS are shown in Figs. 6 to 9. High-grade resource utilization has been reported, and the relative content of each component was determined *via* area normalization.

Figure 10 shows the distribution of all pyrolysis products for the four groups of samples. It reveals that the biogas and bio-oil were prepared by cracking of the sample. According to the PY-GC-MS results for HP1, 64 thermal cracking products were detected. The corresponding percentages of each thermal cracking product corresponds to the mass obtained from cracking of 100 g of raw materials. Among them, for each 100 g of HP1 sample, the thermal cracking products obtained were as follows: 2-butene (8.01 g), 6-hydroxynicotinic acid (6.9 g), toluene (6.31 g), 2-methyl-1-pentene (5.27 g), benzene (4.39 g), 3-penten-1-yne,3-methyl (3.18 g), 1-heptene (3.06 g), 3-methyl-furan (2.49 g), 2,4-dimethylfuran (2.21 g), and 1-pentene (2.08 g).

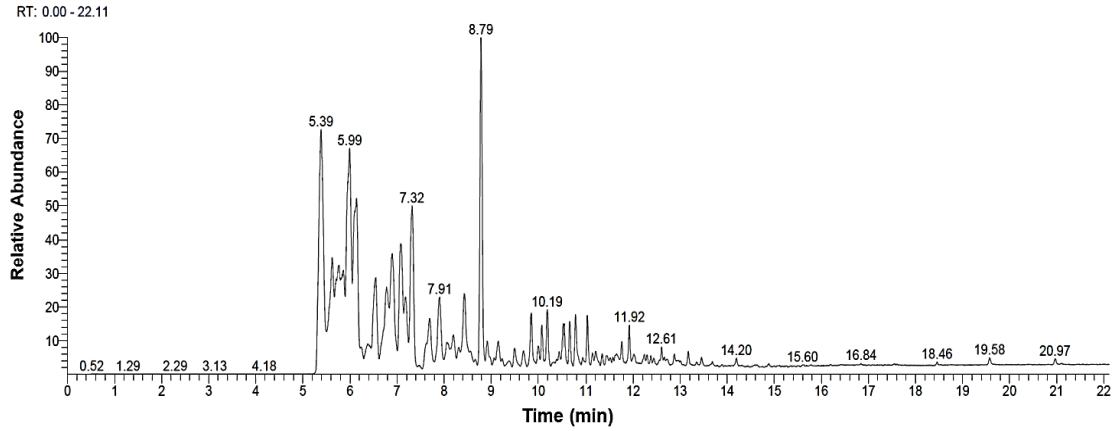

Fig. 6. Total ion current chromatograms of HP1 by PY-GC-MS

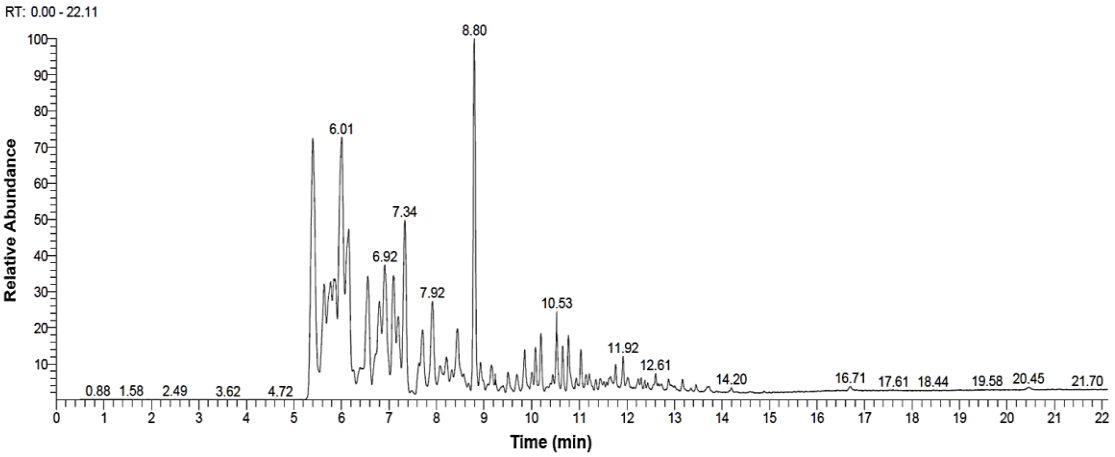

Fig. 7. Total ion current chromatograms of HP2 by PY-GC-MS

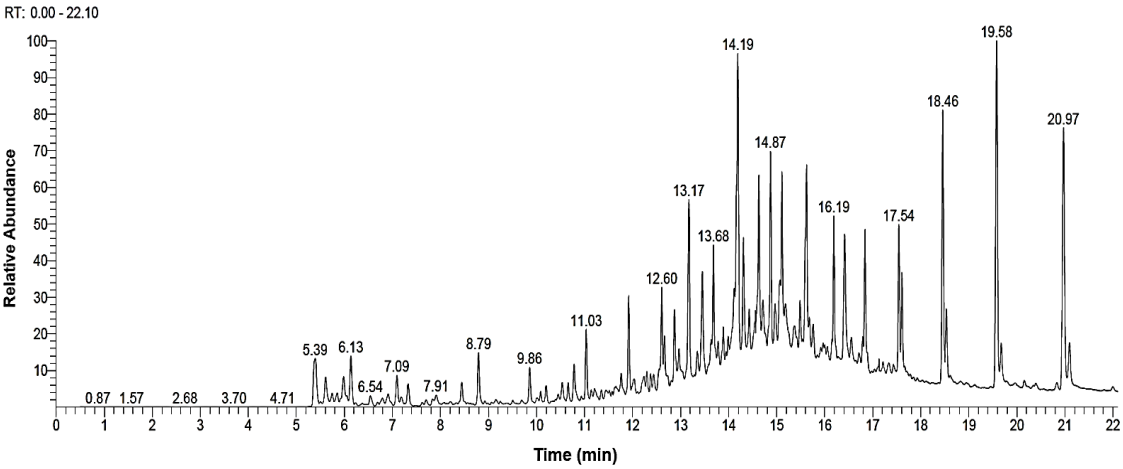

Fig. 8. Total ion current chromatograms of HP3 by PY-GC-MS

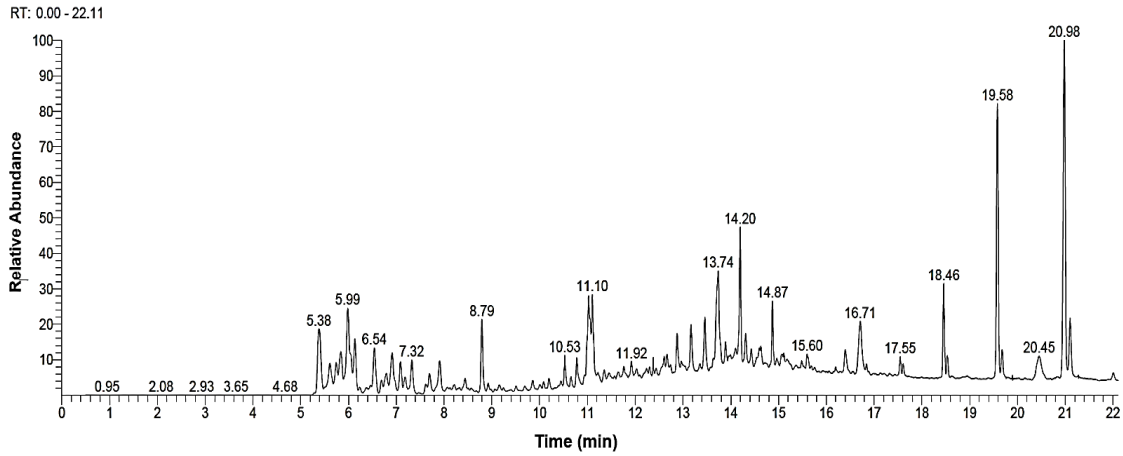

Fig. 9. Total ion current chromatograms of HP4 by PY-GC-MS

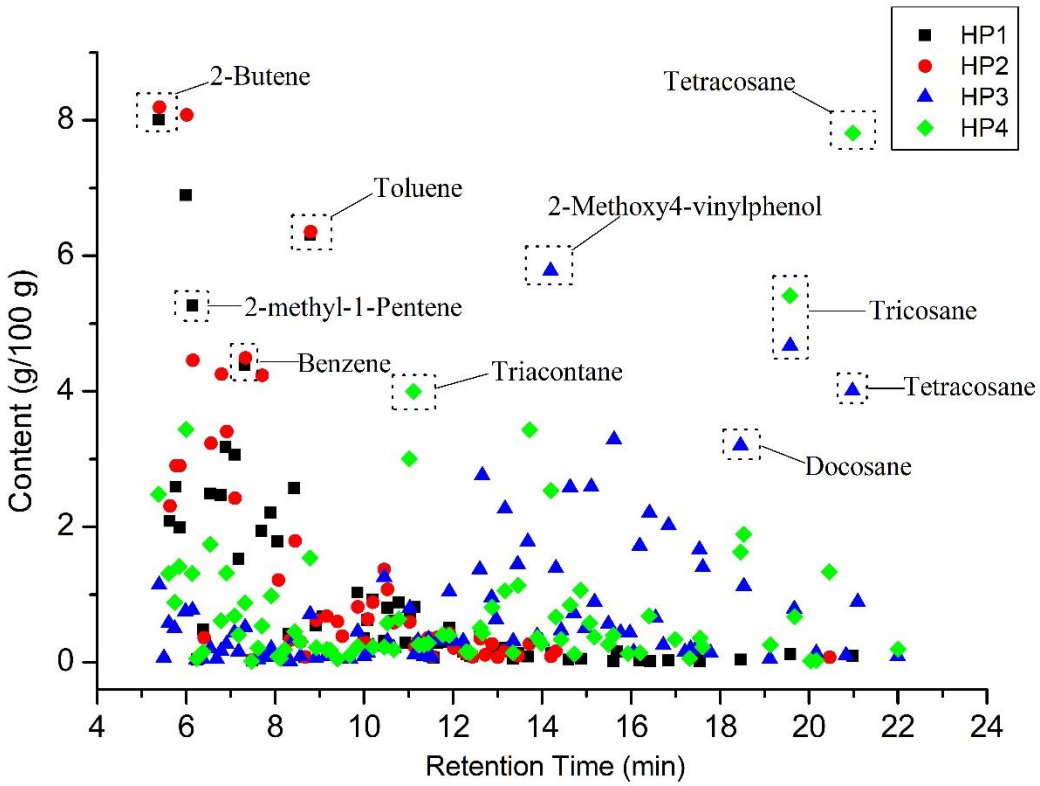

Fig. 10. Pyrolysis product distribution diagram by PY-GC-MS

According to the PY-GC-MS results for HP2, 53 thermal cracking products were detected. Every 100 g of HP2 sample pyrolysed yielded: 2-butene (8.19 g), tetrahydro-3,6-dimethyl-2-H-pyran-2-one (8.08 g), ethylbenzene (6.36 g), cyclopropane (4.49 g), 5-methyl-1,3-cyclopentadiene (4.46 g), cyclobutane (4.26 g), furfural (4.23 g), 1,4-pentadiene (3.41 g), 3-methyl-furan (3.23 g), toluene (2.90 g), 1-heptene (2.42 g), and 6-hydroxynicotinic acid (2.31 g).

According to the PY-GC-MS results for HP3, 90 thermal cracking products were detected. Every 100 g of HP3 sample pyrolysed yielded: 2-methoxy-4-vinylphenol (5.78

g), tricosane (4.67 g), tetracosane (4.01 g), 1-octadecanol (3.29 g), docosane (3.2 g), phenol (2.76 g), cetene (2.59 g), 3-heptadecene (Z) (2.59 g), 1-eicosanol (2.02 g), and 1-hexadecanol (1.78 g).

According to the PY-GC-MS results for HP4, 80 thermal cracking products were detected. Every 100 g of HP4 sample pyrolyzed afforded: Tetracosane (10.77 g), tricosane (7.46 g), triacontane (5.51 g), 6-hydroxynicotinic acid (4.74 g), hexacosane (4.73 g), pentacosane (4.14 g), 2-methoxy-4-vinylphenol (3.5 g), 2-butene (3.42 g), n-tetracosanol (2.6 g), furan-3-methyl (2.4 g), docosane (2.25 g), 1,4-pentadiene (1.95 g), and octacosane (1.84 g).

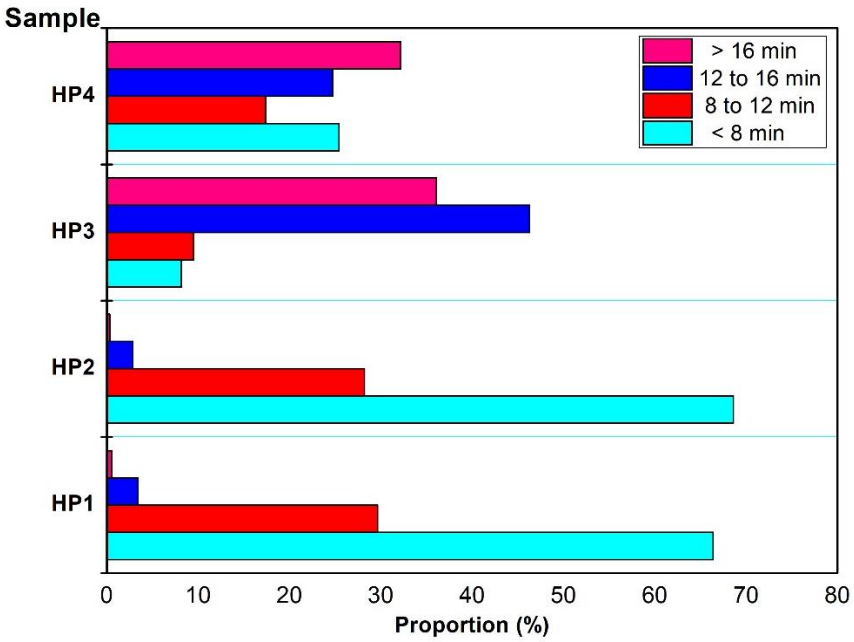

Fig. 11. Distribution characteristic of the sample according to retention time

Figure 11 shows the statistics of the products obtained by thermal cracking of each group of samples according to retention time. As for the HP1 sample, the retention time of the molecular cleavage occurring in less than 8 min accounted for 66.4%, the retention time of the 8 to 12 min molecular cleavage was 29.6%, and that at 12 to 16 min accounted for 3.4%, and the molecular weight with retention time greater than 16 min accounted for 0.5%. For HP2 sample, the molecular cleavage less than 8 min accounted for 68.6%, the retention time at 8 to 12 min, the cleavage was at 28.2%, at 12 to 16 min, the pyrolysis accounted for 2.9%, and at retention time greater than 16 min the occurred at 0.3%. For HP3 sample, at the retention time of less than 8 min the molecular cleavage accounted for 8.2%, at time of 8 to 12 min accounted for 9.5%, at retention time of 12 to 16 min accounted for 46.3%, and the retention time longer than 16 min corresponded to 36.1%. For HP4 sample, at retention time less than 8 min accounted for 25.4%, retention time 8 to 12 min cleavage was at 17.41%, retention time 12 to 16 min molecular weight accounted for 24.7%, and retention time greater than 16 min molecular weight accounted for 32.2%. Through comparing and analyzing the four groups of samples, the molecular weights of cleavage products in HP1 and HP2 mainly were concentrated before the first 12 min, especially during the period of 5 to 10 min. The HP3 and HP4 samples catalyzed the release

of molecules after pyrolysis during 12 min. The HP3 sample released the most products (46.3%) at 12 to 16 min after the addition of Nano-NiO, which was much larger than that of samples HP1 (3.4%) and HP2 (2.9%).

The molecular weight release during pyrolysis of samples HP1 and HP2 was mainly concentrated in 5 to 12 min. The pyrolysis products in this process were mainly: 2-butene, hydroxynicotinic acid, 1-pentene, furan, 1-heptene, 1-nonene, toluene, and the like. Pyrolysis products mainly constitute aliphatic hydrocarbons and unsaturated fatty acids. Among them, aliphatic hydrocarbons are generally important components of oil and natural gas. C1-C5 low-carbon aliphatic hydrocarbons are the basic raw materials for petrochemical industry, especially ethylene and propylene, and C4 and C5 conjugated olefins. These are the most widely used in petrochemical industry (Domańska and Marciniak 2008; Heineman *et al*. 2010; Stroud *et al*. 2010). Unsaturated fatty acids are essential fatty acids that maintain the relative fluidity of the cell membrane to preserve the normal physiological functions of the cells. At the same time, they esterify cholesterol and lower blood cholesterol and triglycerides (Mcphail *et al*. 1984; Lee *et al*. 2001; Wolfe 2010). The low molecular weight compounds released during the pyrolysis of samples HP3 and HP4 were mainly concentrated during the 12 to 20 min period. The pyrolysis products during this time mainly include: creosol, 1-hexadecanol, 2-methoxy-4-vinylphenol, 1-octadecanol, docosane, tricosane, acetic acid, and the like. In addition to aliphatic hydrocarbons, pyrolysis products at this stage mainly contain unsaturated alcohols and phenols. Among them, the presence of creosol, 1-hexadecanol, and 2-methoxy4-vinylphenol illustrates the reason why CNB exudes a special aroma. Acetic acid is an important chemical product that is resistant to bacterial and fungal infections. It is used to treat various bacterial or fungal infections in various skin types. It can also be used for vaginal trichomoniasis, burn wound infection, and prevention of colds or flu and in contraception (Basu *et al*. 2003; Okabe and Amagase 2005).

FTIR Analysis

The FTIR spectrum of CNB was analyzed to understand the relationship between the presence of the organic compounds and their functional groups. Figure 12 shows the IR contrast spectra of CNB extract B1.

As shown in Fig. 12, the absorbance peaks of the extract were mainly concentrated in the regions of 3550 to 3300 cm^{-1}, 1800 cm^{-1}, 500 cm^{-1}, and 1100 to 700 cm^{-1}. An absorbance peak is formed by the oscillation or anti-tensile vibration free hydroxyl groups in liquid water at 3400 cm^{-1} or higher. The absorbance peak found at 3500 to 3350 cm^{-1} due to intermolecular association appeared as a broad peak. An absorbance peak at 2948 cm^{-1} was formed by antisymmetric stretching of the CH_2 group. The absorbance peak at 1869 to 1559 cm^{-1} may be caused by the formation of C=O double bond stretching vibration. The appearance of an absorbance peak at 1450 cm^{-1} indicates the formation of asymmetric angular vibration of CH_3. The absorbance peak at 1170 cm^{-1} is the antisymmetric stretching of the C-O-C of the ester component. The absorbance peak at 1100 cm^{-1} was formed by symmetric and antisymmetric stretchings of C-O-C of esters and ethers. The formation of an absorbance peak at 1020 cm^{-1} was caused by stretching vibration of a C-O bond or asymmetric stretching vibration of a P-O-C bond. The absorbance peak at 700 cm^{-1} was formed by out-of-plane bending of C-OH.

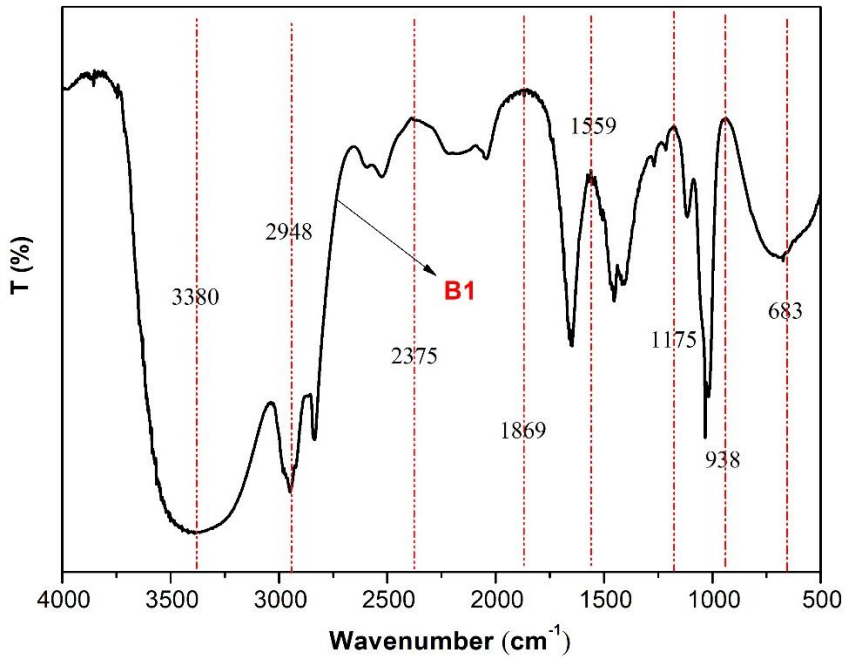

Fig. 12. FTIR spectra of the initial bark

The observed cellulose absorbance peak (3550 to 3300 cm^{-1}) was noticeably lowered, indicating that the cellulose was hydrolyzed. The absorbance peaks of hemicellulose (3000 and 2860 cm^{-1}) and lignin (1480 to 1430 cm^{-1}) were slightly lowered, indicating that the degree of hydrolysis of hemicellulose and lignin was lower than that of cellulose. The absorbance peaks of the extracts were mainly concentrated in the regions of 3550 to 3300 cm^{-1}, 1800 to 1500 cm^{-1}, and 1100 to 700 cm^{-1}. After analysis, the main chemical components observed were terpenoids, phenols, alcohols, acids, ketones, esters, hydrocarbons, and aromatics (Pasquali and Herrera 1997; Carrillo *et al*. 2004; Kim *et al*. 2005; Zhang *et al*. 2006). In addition, a decrease in the characteristic absorbance peak of the organic chemical component indicates that these chemical components were partially extracted.

GC-MS Analysis the Initial Bark Extract

The total ion chromatograms of the B1 extractive analyzed *via* GC-MS are shown in Fig. 13. The spectrum of each peak was retrieved using a computer and the Wiley7n.1 standard spectrum. The peak area normalization method was used to calculate the content of each component (Delazar *et al*. 2004; Čajka *et al*. 2015).

The sample was extracted to obtain liquid biogas and bio-oil. The types and contents of the liquid biogas and bio-oil in the sample extract were detected by GC-MS. According to GC-MS results, 25 compounds were identified. Among them, using an organic solvent to extract 100 g of sample yielded: nonacosane (0.73 g), N,N-diethyl-formamide (0.33 g), 2-ethyl-1-hexanol (0.26 g), triacontane (0.49 g), 4-androstene-3,17-dione 17-mono (O-methyloxime) (0.18 g), 17-pentatriacontene (0.09 g), azafrin (0.08 g), octadecane (0.06 g), n-hexadecanoic acid (0.02 g), phthalic acid (0.01 g), oleic acid (0.01 g), tetracosane (0.05 g), bacteriochlorophyll-C-stearyl (0.05 g), butanoic acid (0.02 g), and 3-ethyl-5-(2-ethylbutyl)-octadecane (0.05 g).

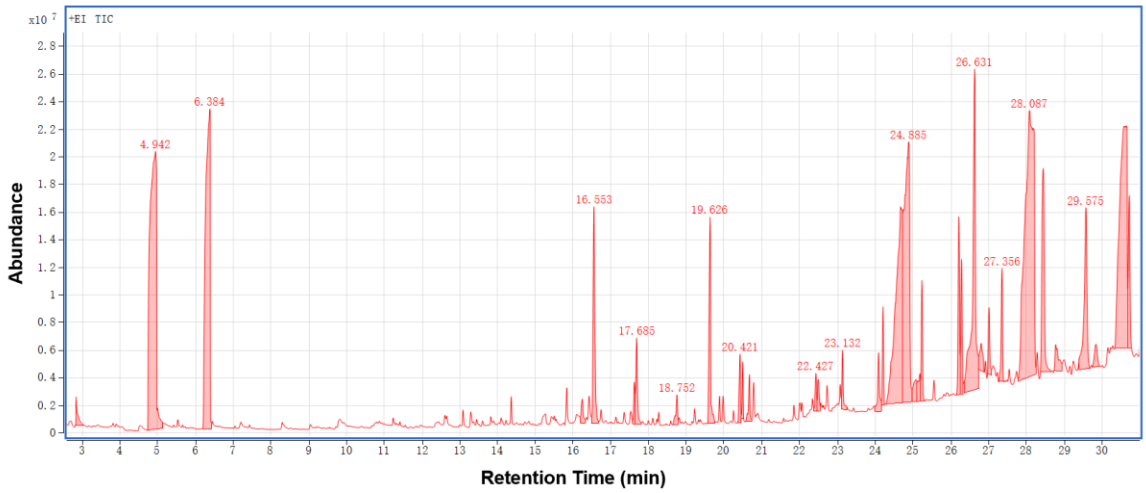

Fig. 13. Total ion chromatograms of the B1 extract

Among the extracted liquid biogas and bio-oil, N,N-diethylformamide has active reactivity and special solubility. It can be used as raw material in organic synthesis, paper treatment agent, softener in fiber industry, softener for animal glue, and to determine amino acids content in rice. Apart from analytical reagent in organic synthesis, there are many uses in medicine, pesticides, dyes, pigments, perfumes, and auxiliaries. It is also an excellent organic solvent, mainly used in spinning and ion exchange resins of acrylonitrile copolymers, as well as antistatic or conductive coatings of plastic products (Sharkawi 1979; Fail *et al*. 1998). The main purpose of butyric acid is to manufacture cellulose butyrate, which is important in the manufacture of food packaging, glasses, automobile steering wheels, black telephone parts, *etc*. The cellulose butyrate is stronger than cellulose acetate in terms of anti-aging, water resistance, and shrinkage. Acids are also widely used in the manufacture of varnishes and molding powders. It can be used not only as a raw material for butter, cheese, and spices, but also for flavoring and thickening in many fruit flavors. When used as a fragrance, a small amount of butyric acid can be used to emit a strong odor (Morley 1980; Slaughter *et al*. 1981; Nudelman *et al*. 1992). Oleic acid is an unsaturated fatty acid containing a carbon-carbon double bond in its molecular structure and is a fatty acid constituting olein. Oleic acid is commonly used in soaps, lubricants, flotation agents, and ointments. The oleate is a good solvent for fatty acids and oil-soluble substances. Oleic acid has cis-trans isomers. Natural oleic acid is a cis-structure. It has a certain effect on softening blood vessels and plays an important role in the metabolism of humans and animals (Horton *et al*. 2002; Minokoshi *et al*. 2002). However, the body's own synthetic oleic acid cannot meet the needs. Hence, it needs to be taken from food, and it is good to use cooking oil with a high oleic acid content.

Biomass produces bio-oil and other biochemicals that have huge application potential and economic value. Nanocatalysts are promising agents in the proliferation of the product during the pyrolysis of *Cotinus nana* bark. In the future, the process parameters, such as thermal efficiency, catalyst type, and catalyst particle size and amount, to maximize the pyrolysis, improve total yield and production performance should be evaluated.

CONCLUSIONS AND PERSPECTIVES

1. Thermogravimetric tests showed that *Cotinus nana* bark produced some volatile compounds in the pyrolysis process, including acids, hydrocarbons, aldehydes, ketones, and alcohols. They are an important component of bio-oil. During the pyrolysis process, the non-covalent bond molecules in the sample particles were destroyed, and a large amount of volatilization and combustion occurred that was analyzed.
2. The nanocatalyst NiO catalyzed the pyrolysis of the bark, and it accelerated the precipitation of the volatile component. The PY-GC/MS test showed that the molecular weights of the thermal cracking products from bark were different with different catalysts. After adding nano NiO, the sample released the maximum low molecular components in 12 to16 min. The pyrolysis products of this process include creosol, 1-hexadecanol, 2-methoxy-4-vinylphenol, 1-octadecanol, acetic acid, *etc*. These can be used as bio-oil raw materials. Samples containing nano NiO showed a good catalytic effect on pyrolysis.
3. Both FTIR and GC-MS results revealed some of the features of the bark extract. The absorption peaks of the extract were mainly concentrated in the 3550 to 3300 cm^{-1}, 1800 to 1500 cm^{-1}, and 1100 to 700 cm^{-1} regions. After analysis, the main chemical components were terpenoids, phenols, alcohols, acids, ketones, esters, and aromatics. These products are not only widely used in various industries, but also in medicine.

Declaration of Competing Interest

The authors declare that they have no known competing financial interests or personal relationships.

ACKNOWLEDGEMENTS

This study was supported by the Program for Innovative Research Team (in Science and Technology) in University of Henan Province (No. 21IRTSTHN020), and Central Plain Scholar Funding Project of Henan Province (No. 212101510005).

REFERENCES CITED

An, Y. R., Fan, X. L., Luo, Z. F., and Lau, W. M. (2017). "Nanopolygons of monolayer MS2: Best morphology and size for HER catalysis," *Nano Letters* 17(1), 368-376. DOI: 10.1021/acs.nanolett.6b04324

Banerjee, I., De, K., Mukherjee, D., Dey, G., Chattopadhyay, S., Mukherjee, M., Mandal, M., Bandyopadhyay, A. K., Gupta, A., Ganguly, S., *et al*. (2016). "Paclitaxel-loaded solid lipid nanoparticles modified with Tyr-3-octreotide for enhanced anti-angiogenic and anti-glioma therapy," *Acta Biomaterialia* 38, 69-81. DOI: 10.1016/j.actbio.2016.04.026

Baruah, D., Das, R. N., Hazarika, S., and Konwar, D. (2015). "Biogenic synthesis of cellulose supported Pd(0) nanoparticles using hearth wood extract of *Artocarpus*

lakoocha Roxb — A green, efficient and versatile catalyst for Suzuki and Heck coupling in water under microwave heating," *Catalysis Communications* 72, 73-80. DOI: 10.1016/j.catcom.2015.09.011

Bassilakis, R., Carangelo, R. M., and Wójtowicz, M. A. (2001). "TG-FTIR analysis of biomass pyrolysis," *Fuel* 80(12), 1765-1786. DOI: 10.1016/S0016-2361(01)00061-8

Basu, P. S., Sankaranarayanan, R., Mandal, R., Roy, C., Das, P., Choudhury, D., Bhattacharya, D., Chatterjee, R., Dutta, K., Barik, S., *et al.* (2003). "Visual inspection with acetic acid and cytology in the early detection of cervical neoplasia in Kolkata, India," *International Journal of Gynecological Cancer* 13(5), 626-632. DOI: 10.1046/j.1525-1438.2003.13394.x

Byler, D. M., and Susi, H. (2010). "Examination of the secondary structure of proteins by deconvolved FTIR spectra," *Biopolymers* 25(3), 469-487. DOI: 10.1002/bip.360250307

Čajka, T., Maštovská, K., Lehotay, S. J., and Hajšlová, J. (2015). "Use of automated direct sample introduction with analyte protectants in the GC–MS analysis of pesticide residues," *Journal of Separation Science* 28(9-10), 1048-1060. DOI: 10.1002/jssc.200500050

Camacho, N. P., West, P., Torzilli, P. A., and Mendelsohn, R. (2015). "FTIR microscopic imaging of collagen and proteoglycan in bovine cartilage," *Biopolymers* 62(1), 1-8. DOI: 10.1002/1097-0282(2001)62:1<1::AID-BIP10>3.0.CO;2-O

Carrillo, F., Colom, X., Sunol, J. J., and Saurina, J. (2004). "Structural FTIR analysis and thermal characterisation of lyocell and viscose-type fibres," *European Polymer Journal* 40(9), 2229-2234. DOI: 10.1016/j.eurpolymj.2004.05.003

Chen, D. Y., Zhou, J. B., and Zhang, Q. S. (2014). "Effects of torrefaction on the pyrolysis behavior and bio-oil properties of rice husk by using TG-FTIR and Py-GC/MS," *Energy & Fuels* 28(9), 5857-5863. DOI: 10.1021/ef501189p

Chen, G., Andries, J., Luo, Z., and Spliethoff, H. (2003). "Biomass pyrolysis/gasification for product gas production: The overall investigation of parametric effects," *Energy Conversion and Management* 44(11), 1875-1884. DOI: 10.1016/S0196-8904(02)00188-7

Dauner, M., and Sauer, U. (2010). "GC-MS analysis of amino acids rapidly provides rich information for isotopomer balancing," *Biotechnology Progress* 16(4), 642-649. DOI: 10.1021/bp000058h

Delazar, A., Reid, R. G., and Sarker, S. D. (2004). "GC-MS analysis of the essential oil from the oleoresin of *Pistacia atlantica*, var. *mutica*," *Chemistry of Natural Compounds* 40(1), 24-27. DOI: 10.1023/B:CONC.0000025459.72590.9e

Demirci, B., Demirci, F., and Baser, K. H. C. (2003). "Composition of the essential oil of *Cotinus coggygria* Scop. from Turkey," *Flavour and Fragrance Journal* 18(1), 43-44. DOI: 10.1002/ffj.1149

Domańska, U., and Marciniak, A. (2008). "Measurements of activity coefficients at infinite dilution of aromatic and aliphatic hydrocarbons, alcohols, and water in the new ionic liquid [EMIM][SCN] using GLC," *Journal of Chemical Thermodynamics* 40(5), 860-866. DOI: 10.1016/j.jct.2008.01.004

Dong, J., Li, F., and Xie, K. (2012). "Study on the source of polycyclic aromatic hydrocarbons (PAHs) during coal pyrolysis by PY-GC-MS," *Journal of Hazardous Materials* 243, 80-85. DOI: 10.1016/j.jhazmat.2012.09.073

Doss, M. A., Rajarajan, G., Thanikachalam, V., Selvanayagam, S., and Sridhar, B. (2017). "Synthesis, spectroscopic (UV-Vis, FT-IR and NMR), single crystal XRD of

3,5-diethyl-2,6-di(thiophen-2-yl)piperidin-4-on-1-ium picrate: A comprehensive experimental and computational study," *Journal of Molecular Structure* 1128, 268-278. DOI: 10.1016/j.molstruc.2016.08.065

Ephraim, A., Minh, D. P., Lebonnois, D., Peregrina, C., Sharrock, P., and Nzihou, A. (2018). "Co-pyrolysis of wood and plastics: Influence of plastic type and content on product yield, gas composition and quality," *Fuel* 231, 110-117. DOI: 10.1016/j.fuel.2018.04.140

Fail, P. A., George, J. D., Grizzle, T. B., and Heindel, J. J. (1998). "Formamide and dimethylformamide: Reproductive assessment by continuous breeding in mice," *Reproductive Toxicology* 12(3), 317-332. DOI: 10.1016/S0890-6238(98)00011-2

Fischer, E., and Sauer, U. (2003). "Metabolic flux profiling of *Escherichia coli*, mutants in central carbon metabolism using GC-MS," *Journal of Biochemistry* 270(5), 880-891. DOI: 10.1046/j.1432-1033.2003.03448.x

Ge, S. B., Liang, Y. Y., Zhou, C. X., Sheng, Y. Q., Zhang, M. L., *et al.* (2022). "The potential of *Pinus armandii* Franch for high-grade resource utilization," *Biomass & Bioenergy* 158, article 106345. DOI: 10.1016/j.biombioe.2022.106345

Gu, H. D., Tang, Y. Z., Yao, J., and Chen, F. (2018). "Study on biomass gasification under various operating conditions," *Journal of the Energy Institute* 92(5), 1329-1336. DOI: 10.1016/j.joei.2018.10.002

Haykiri-Acma, H., Yaman, S., and Kucukbayrak, S. (2006). "Effect of heating rate on the pyrolysis yields of rapeseed," *Renewable Energy* 31(6), 803-810. DOI: 10.1016/j.renene.2005.03.013

He, Z. J., Wan, X. M., Schulz, A., Bludau, H., Dobrovolskaia, M. A., Stern, S. T., Montgomery, S. A., Yuan, H., Li, Z. B., Alakhova, D., *et al.* (2016). "A high capacity polymeric micelle of paclitaxel: Implication of high dose drug therapy to safety and *in vivo* anti-cancer activity," *Biomaterials* 101, 296-309. DOI: 10.1016/j.biomaterials.2016.06.002

Heineman, E. F., Cocco, P., Gómez, M. R., Dosemeci, M., Stewart, P. A., and Hayes, R. B. (2010). "Occupational exposure to chlorinated aliphatic hydrocarbons and risk of astrocytic brain cancer," *American Journal of Industrial Medicine* 26(2), 155-169. DOI: 10.1002/ajim.4700260203

Horton, J. D., Goldstein, J. L., and Brown, M. S. (2002). "SREBPs: Activators of the complete program of cholesterol and fatty acid synthesis in the liver," *Journal of Clinical Investigation* 109(9), 1125-1131. DOI: 10.1172/JCI15593

Ilczuk, A., and Jacygrad, E. (2016). "The effect of IBA on anatomical changes and antioxidant enzyme activity during the in vitro rooting of smoke tree (*Cotinus coggygria* Scop.)," *Scientia Horticulturae* 210, 268-276. DOI: 10.1016/j.scienta.2016.07.036

Ivanova D., Gerova D., Chervenkov T., Yankova, T. (2005) "Polyphenols and antioxidant capacity of Bulgarian medicinal plants," *Journal of Ethnopharmacology*, 96(1-2), 145-150. DOI: 10.1016/j.jep.2004.08.033

Jassbi, A. R., Zamanizadehnajari, S., Azar, P. A., and Tahara, S. (2002) "Antibacterial Diterpenoids from Astragalus brachystachys." *Zeitschrift Fur Naturforschung Section C-a Journal of Biosciences* 57, 11-12. DOI: 10.1515/znc-2002-11-1211.

Jiang, S. C., Ge, S. B., and Peng, W. X. (2017). "Molecules and functions of rosewood: *Dalbergia stevenson*," *Arabian Journal of Chemistry* 11(6), 782-792. DOI: 10.1016/j.arabjc.2017.12.032

Jiang, X. G., Li, C. Y., Chi, Y., and Yan, J. H. (2010). "TG-FTIR study on urea-formaldehyde resin residue during pyrolysis and combustion," *Journal of Hazardous Materials* 173(1-3), 205-210. DOI: 10.1016/j.jhazmat.2009.08.070

Jong, W. D., Pirone, A., and Wójtowicz, M. A. (2003). "Pyrolysis of *Miscanthus giganteus* and wood pellets: TG-FTIR analysis and reaction kinetics," *Fuel* 82(9), 1139-1147. DOI: 10.1016/S0016-2361(02)00419-2

Kaal, J., Nierop, K. G. J., Kraal, P., and Preston, C. M. (2012). "A first step towards identification of tannin-derived black carbon: Conventional pyrolysis (PY-GC-MS) and thermally assisted hydrolysis and methylation (THM-GC-MS) of charred condensed tannins," *Organic Geochemistry* 47(6), 99-108. DOI: 10.1016/j.orggeochem.2012.03.009

Kim, B., Lee, C., Lee, E. S., Shin, B. S., and Youn, Y. S. (2016). "Paclitaxel and curcumin co-bound albumin nanoparticles having antitumor potential to pancreatic cancer," *Asian Journal of Pharmaceutical Sciences* 11(6), 708-714. DOI: 10.1016/j.ajps.2016.05.005

Kim, J. S. (2013). "FT-IR, XRD, and TGA-DTA characterization of melanoidins formed from black garlic at different thermal processing steps," *Acta Psychiatrica Scandinavica* 96(2), 155-156. DOI: 10.1111/j.1600-0447.1997.tb09921.x

Kim, J., Lee, J., Choi, H., Sohn, D., and Ahn, D. J. (2005). "Rational design and *in-situ* FTIR analyses of colorimetrically reversible polydiacetylene supramolecule," *Macromolecules* 38(22), 9366-9376. DOI: 10.1021/ma051551i

Lee, J. Y., Sohn, K. H., Rhee, S. H., and Hwang, D. (2001). "Saturated fatty acids, but not unsaturated fatty acids, induce the expression of cyclooxygenase-2 mediated through toll-like receptor 4," *Journal of Biological Chemistry* 276(20), 16683-16689. DOI: 10.1074/jbc.M011695200

Lei, Y. K., Wang, W., Liu, Y. P., He, D., and Li, Y. (2015). "Adaptive genetic variation in the smoke tree (*Cotinus coggygria* Scop.) is driven by precipitation," *Biochemical Systematics and Ecology* 59, 63-69. DOI: 10.1016/j.bse.2015.01.009

Liu, B., Yan, P., Xu, W., Zheng, J. M., He, Y., Luo, L. L., Bowden, M. E., Wang, C. M., and Zhang, J. G. (2016). "Electrochemically formed ultrafine metal oxide nanocatalysts for high-performance lithium-oxygen batteries," *Nano Letters* 16(8), 4932-4939. DOI: 10.1021/acs.nanolett.6b01556

Luís, Â., Neiva, D. M., Pereira, H., Gominho, J., Domingues, F., and Duarte, A. P. (2016). "Bioassay-guided fractionation, GC–MS identification and *in vitro* evaluation of antioxidant and antimicrobial activities of bioactive compounds from *Eucalyptus globulus* stump wood methanolic extract," *Industrial Crops and Products* 91, 97-103. DOI: 10.1016/j.indcrop.2016.06.022

Mahmoud, M. A., Saira, F., and Elsayed, M. A. (2010). "Experimental evidence for the nanocage effect in catalysis with hollow nanoparticles," *Nano Letters* 10(9), 3764-3769. DOI: 10.1021/nl102497u

Marcetic, M., Bozic, D., Milenkovic, M., Malesevic, N., Radulovic, S., and Kovacevic, N. (2012). "Antimicrobial, antioxidant and anti-inflammatory activity of young shoots of the smoke tree, *Cotinus coggygria* Scop.," *Phytotherapy Research* 27(11), 1658-1663. DOI: 10.1002/ptr.4919

Matic, S., Stanic, S., Bogojevic, D., Solujic, S., Grdovic, N., Vidakovic, M., and Mihailovic, M. (2011). "Genotoxic potential of *Cotinus coggygria* Scop. (Anacardiaceae) stem extract *in vivo*," *Genetics and Molecular Biology* 34(2), 298-303. DOI: 10.1590/S1415-47572011005000001

Matic, S., Stanic, S., Bogojević, D., Vidaković, M., Grdović, N., Dinić, S., Solujić, S., Mladenović, M., Stanković, N., and Mihailović, M. (2013). "Methanol extract from the stem of *Cotinus coggygria* Scop., and its major bioactive phytochemical constituent myricetin modulate pyrogallol-induced DNA damage and liver injury," *Mutation Research/Genetic Toxicology and Environmental Mutagenesis* 755(2), 81-89. DOI: 10.1016/j.mrgentox.2013.03.011

Matic, S., Stanic, S., Mihailovic, M., and Bogojevic, D. (2016). "*Cotinus coggygria* Scop.: An overview of its chemical constituents, pharmacological and toxicological potential," *Saudi Journal of Biological Sciences* 23(4), 452-461. DOI: 10.1016/j.sjbs.2015.05.012

McPhail, L. C., Clayton, C. C., and Snyderman, R. (1984). "A potential second messenger role for unsaturated fatty acids: Activation of Ca^{2+} dependent protein kinase," *Science* 224(4649), 622-625. DOI: 10.1126/science.6231726

Meent, D. V. D., Brown, S. C., Philp, R. P., and Simoneit, B. (1980). "Pyrolysis-high resolution gas chromatography and pyrolysis gas chromatography-mass spectrometry of kerogens and kerogen precursors," *Geochimica et Cosmochimica Acta* 44(7), 999-1013. DOI: 10.1016/0016-7037(80)90288-4

Mekonnen, D., Bryan, E., Alemu, T., and Ringler, C. (2017). "Food *versus* fuel: Examining tradeoffs in the allocation of biomass energy sources to domestic and productive uses in Ethiopia," *Agricultural Economics* 48(4), 425-435. DOI: 10.1111/agec.12344

Minokoshi, Y., Kim, Y. B., Peroni, O. D., Fryer, L. G. D., Muller, C., Carling, D., and Kahn, B. B. (2002). "Leptin stimulates fatty-acid oxidation by activating AMP-activated protein kinase," *Nature* 415(6869), 339-343. DOI: 10.1038/415339a

Morley, J. E. (1980). "The neuroendocrine control of appetite: The role of the endogenous opiates, cholecystokinin, TRH, gamma-amino-butyric-acid and the diazepam receptor," *Life Science* 27(5), 355-368. DOI: 10.1016/0024-3205(80)90183-6

Mullen, C. A., Boateng, A. A., and Goldberg, N. M. (2013). "Production of deoxygenated biomass fast pyrolysis oils *via* product gas recycling," *Energy & Fuels* 27(7), 3867-3874. DOI: 10.1021/ef400739u

Nudelman, A., Ruse, M., Aviram, A., Rabizadeh, E., Shaklai, M., Zimrah, Y., and Rephaeli, A. (1992). "Novel anticancer prodrugs of butyric acid," *Journal of Medicinal Chemistry* 35(4), 687-694. DOI: 10.1021/jm00082a009

Okabe, S., and Amagase, K. (2005). "An overview of acetic acid ulcer models--The history and state of the art of peptic ulcer research," *Biological and Pharmaceutical Bulletin* 28(8), 1321-1341. DOI: 10.1248/bpb.28.1321

Onay, O. (2007). "Influence of pyrolysis temperature and heating rate on the production of bio-oil and char from safflower seed by pyrolysis, using a well-swept fixed-bed reactor," *Fuel Processing Technology* 88(5), 523-531. DOI: 10.1016/j.fuproc.2007.01.001

Pasquali, C., and Herrera, H. (1997). "Pyrolysis of lignin and IR analysis of residues," *Thermochimica Acta* 293(1-2), 39-46. DOI: 10.1016/S0040-6031(97)00059-2

Peng, W. X., Lin, Z., Wang, L. S., Chang, J. B., Gu, F. L., and Zhu, X. W. (2016). "Molecular characteristics of *Illicium verum* extractives to activate acquired immune response," *Saudi Journal of Biological Sciences* 23(3), 348-352. DOI: 10.1016/j.sjbs.2015.10.027

Reddy, V., Urooj, A., and Kumar, A. (2005). "Evaluation of antioxidant activity of some plant extracts and their application in biscuits," *Food Chemistry* 90(1-2), 317-321. DOI: 10.1016/j.foodchem.2004.05.038

Sánchez-Gómez, R., Garde-Cerdán, T., Zalacain, A., Garcia, R., Cabrita, M. J., and Salinas. M. R. (2016). "Vine-shoot waste aqueous extract applied as foliar fertilizer to grapevines: Effect on amino acids and fermentative volatile content," *Food Chemistry* 197, 132-140. DOI: 10.1016/j.foodchem.2015.10.034

Sharkawi, M. (1979). "Inhibition of alcohol dehydrogenase by dimethyl formamide and dimethyl sulfoxide," *Toxicology Letters* 4(6), 493-497. DOI: 10.1016/0378-4274(79)90117-6

Si, L. L., Fan, Y., Wang, Y. K., Sun, L. L., Li, B. F., Xue, C. H., and Hou, H. (2018). "Thermal degradation behavior of collagen from sea cucumber (*Stichopus japonicus*) using TG-FTIR analysis," *Thermochimica Acta* 659, 166-171. DOI: 10.1016/j.tca.2017.12.004

Slaughter, M. M., and Miller, R. F. (1981). "2-Amino-4-phosphonobutyric acid: A new pharmacological tool for retina research," *Science* 211(4478), 182-185. DOI: 10.1126/science.6255566

Stroud, J. L., Paton, G. I., and Semple, K. T. (2010). "Microbe-aliphatic hydrocarbon interactions in soil: Implications for biodegradation and bioremediation," *Journal of Applied Microbiology* 102(5), 1239-1253. DOI: 10.1111/j.1365-2672.2007.03401.x

Tian, L., Shen, B., Xu, H., Li, F., Wang, Y., and Singh, S. (2016). "Thermal behavior of waste tea pyrolysis by TG-FTIR analysis," *Energy* 103, 533-542. DOI: 10.1016/j.energy.2016.03.022

Wang, Q., Wang, G., Zhang, J., Lee, J. Y., Wang, H., and Wang, C. (2008). "Combustion behaviors and kinetics analysis of coal, biomass and plastic," *Thermochimica Acta* 669, 140-148. DOI: 10.1016/j.tca.2018.09.016

Wiklund, C. M., Helle, M., Kohl, T., Jarvinen, M., and Saxen, H. (2017). "Feasibility study of woody-biomass use in a steel plant through process integration," *Journal of Cleaner Production* 142, 4127-4141. DOI: 10.1016/j.jclepro.2016.09.210

Williams, P. T., and Besler, S. (1996). "The influence of temperature and heating rate on the slow pyrolysis of biomass," *Renewable Energy* 7(3), 233-250. DOI: 10.1016/0960-1481(96)00006-7

Wolfe, L. S. (2010). "Eicosanoids: Prostaglandins, thromboxanes, leukotrienes, and other derivatives of carbon-20 unsaturated fatty acids," *Journal of Neurochemistry* 38(1), 1-14. DOI: 10.1111/j.1471-4159.1982.tb10847.x

Xue, J. J., Zhuo, J. K., Liu, M., Chi, Y. C., Zhang, D. H., and Yao, Q. (2017). "Synergetic effect of co-pyrolysis of cellulose and polypropylene over an all-silica mesoporous catalyst MCM-41 using thermogravimetry-Fourier transform infrared spectroscopy and pyrolysis gas chromatography-mass spectrometry," *Energy & Fuels* 31(9), 9576-9584. DOI: 10.1021/acs.energyfuels.7b01651

Yu, B. D., Tan, L., Zheng, R. H., Tan, H., and Zheng, L. X. (2016). "Targeted delivery and controlled release of Paclitaxel for the treatment of lung cancer using single-walled carbon nanotubes," *Materials Science and Engineering C* 68, 579-584. DOI: 10.1016/j.msec.2016.06.025

Zhang, Y., Chen, S. S., Qu, F. Z., Su, G. Y., and Zhao, Y. Q. (2019). "*In vivo* and *in vitro* evaluation of hair growth potential of *Cacumen platycladi*, and GC-MS analysis of the active constituents of volatile oil," *Journal of Ethnopharmacology* 238, article ID 111835. DOI: 10.1016/j.jep.2019.111835

Zhang, Z., Zheng, Y. J., Ni, Y. W., Liu, Z. M., Chen, J. P., and Liang, X. M. (2006). "Temperature- and pH-dependent morphology and FT-IR analysis of magnesium carbonate hydrates," *Journal of Physical Chemistry B* 110(26), 12969-12973. DOI: 10.1021/jp061261j

Zhu, H. M., Yan, J. H., Jiang, X. G., Lai, Y. E., and Cen, K. F. (2008). "Study on pyrolysis of typical medical waste materials by using TG-FTIR analysis," *Journal of Hazardous Materials* 153(1-2), 670-676. DOI: 10.1016/j.jhazmat.2007.09.011

Zodrow, E. L., and Mastalerz, M. (2002). "FTIR and PY-GC-MS spectra of true-fern and seed-fern sphenopterids (Sydney Coalfield, Nova Scotia, Canada, Pennsylvanian)," *International Journal of Coal Geology* 51(2), 111-127. DOI: 10.1016/S0166-5162(02)00086-1

Article submitted: March 21, 2022; Peer review completed: June 19, 2022; Revised version received and accepted: November 9, 2022; Published: November 23, 2022.
DOI: 10.15376/biores.18.1.678-700